JOURNAL OF ENVIRONMENTAL SCIENCES 152 (2025) 302–312

Available online at www.sciencedirect.com

ScienceDirect

www.elsevier.com/locate/jes

JES JOURNAL OF ENVIRONMENTAL SCIENCES

www.jesc.ac.cn

Research Article

Modelling and prediction of toluene adsorption saturation basing on characteristic values of activated carbons

Quanli Ke[1], *Yedong Xiong*[1], *Mei Lu*[2], *Kangkang Huang*[1], *Yiting Guo*[1], *Jiong Min*[3], *Chuanmin Jin*[3], *Zhenyu Gu*[4,5], *Guokai Cui*[1], *Xiaole Weng*[5], *Bingzhi Yi*[6], *Hanfeng Lu*[1,*]

[1] *Institute of Catalytic Reaction Engineering, College of Chemical Engineering, Zhejiang University of Technology, Hangzhou 310014, China*
[2] *Zhejiang Environmental Technology Co., Ltd., Hangzhou 311121, China*
[3] *Joint Research Center with ZJUT, Zhejiang Yuesheng Environmental Technology Co., Ltd., Huzhou 313300, China*
[4] *Eco-environmental Science Research & Design Institute of Zhejiang Province, Hangzhou 310007, China*
[5] *College of Environmental and Resource Sciences, Zhejiang University, Hangzhou 310058, China*
[6] *School of Materials Science and Engineering, Zhejiang Sci-Tech University, Hangzhou 310018, China*

ARTICLE INFO

Article history:
Received 14 March 2024
Revised 24 April 2024
Accepted 24 April 2024
Available online 3 May 2024

Keywords:
Activated carbon
Adsorption
Characteristic values
Toluene saturation
Modelling

ABSTRACT

Herein, the association between the dynamic adsorption capacity of toluene and several important characteristic values on activated carbon (AC) samples was investigated by multidimensional linear regression. Among the characteristic values, the carbon tetrachloride (CTC) adsorption value has demonstrated relatively stronger correlation with the toluene adsorption capacity on AC samples with diverse sources and forms, particularly in exposure to high-concentration toluene. Notably, the relevance of the toluene adsorption capacity to the CTC value could also be extended to a series of other porous adsorbents, which proved the wide applicability of CTC value in characterizing the adsorption behaviors. Based on these results, a mathematical and visual model was then established to predict the toluene adsorption saturation under different conditions (inlet concentration, adsorption time, initial CTC value, etc.) on diverse AC samples, of which the accuracy has later been verified by experimental data. As such, a fast and accurate estimation of the adsorption behaviors over AC samples, and possibly other porous adsorbents, was realized.

© 2024 The Research Center for Eco-Environmental Sciences, Chinese Academy of Sciences. Published by Elsevier B.V.

* Corresponding author.
E-mail: luhf@zjut.edu.cn (H. Lu).

https://doi.org/10.1016/j.jes.2024.04.039
1001-0742/© 2024 The Research Center for Eco-Environmental Sciences, Chinese Academy of Sciences. Published by Elsevier B.V.

Introduction

Volatile organic compounds (VOCs) are considered as organic contaminants, which may not only pose serious risks to human health even at diluted concentrations (Liang et al., 2024; Lin et al., 2023; Soni et al., 2018), but also generate harmful environmental hazards such as photochemical smog, organic aerosols, etc. (Tan et al., 2023; Zhang et al., 2020a). Moreover, in term of the VOCs emission sources features, it could be noted that the low concentration (generally at ppm level), high flow rate and severe concentration fluctuation of the VOCs-containing streams are the hardest nuts to crack, which severely interfere with the removal efficiency (Ye et al., 2023). Currently, the VOCs abatement methods could be mainly divided into two categories, namely the elimination and the recovery methods. The elimination methods include thermal/catalytic oxidation, plasma oxidation, photocatalysis, and biodegradation (Dai et al., 2021; Shi et al., 2023; Sun et al., 2024). However, the thermal/catalytic oxidation could easily cause concerns about the energy consumption and catalyst deactivation (especially the noble-metal catalysts), while the scale-up applications of plasma oxidation, photocatalysis, and biodegradation are badly limited by the secondary pollution, long-term efficiency, and rigorous operation conditions, respectively, in practical situations (He et al., 2019; Ji et al., 2017; Wu et al., 2023; Yang et al., 2023; Zhang et al., 2016; Zhou et al., 2016). In consideration of the efficiency and costs of the elimination methods, the recovery methods, such as ab(d)sorption, condensation and membrane separation, seem more sustainable (Algrim et al., 2020; Hao et al., 2021; Shen, 2023; Xiang et al., 2020). Therein, the adsorption method has received widespread attention due to its feasible operation, fast kinetics, low energy consumption and minor risks of external contamination (Yang et al., 2019; Zhu et al., 2020).

Adsorbent, as the core of adsorption method, is directly related to the capacity and selectivity toward VOCs. Hitherto, a variety of porous adsorbents have already been used in VOCs removal, wherein the most prevalent ones are activated carbons (ACs), zeolites and metal-organic framework (MOFs), etc. (Li et al., 2020; Ouzzine et al., 2019; Rao et al., 2023; Yu et al., 2024). Compared to other kinds of porous adsorbents, ACs are extremely preferred for the treatments of low-concentration VOCs, owing to their merits including wide raw material sources, low manufacture costs, high surface area and thus superb adsorption capacity (Bradley, 2011; Liu et al., 2023; Wei et al., 2023; Zhang et al., 2022, 2020b). This may also be at the heart of why ACs materials are broadly adopted in the industrial exhaust purification systems. However, while the ACs could be easily prepared by diverse organic compounds (*e.g.* wood, coal, biomass and polymers), their adsorption capacities also vary significantly as a result of different carbonization and activation procedures, which makes it rather difficult to distinguish the quality of the ACs adsorbents.

To address this problem, the typical way is the adoption of some characteristic values (using different probing molecules) to represent the adsorption properties of ACs. Commonly, the characteristic values are sorted by the phase states (gas or liquid phase) of the probing molecules. The gas-phase probing molecules include carbon tetrachloride (CTC) value and butane, while the liquid-phase ones include iodine (iodine number), methylene blue, tannic acid etc.. Among these characteristic values, iodine number is the most widely used index to characterize the adsorption properties of ACs (Garba, 2016; Juhola, 1975), due to the widespread applications of ACs in wastewater treatments and purification for a long term (Goswami and Dey, 2022; Wang et al., 2021). Nevertheless, regarding the VOCs adsorption using ACs adsorbents, two problems are still remaining. The first one is whether it is reasonable to predict the gas-phase (VOCs) adsorption properties of ACs by a liquid-phase index (*i.e.* iodine number). Next to that, the characteristic values normally serve as some kind of quality standards of fresh samples; however, the ACs adsorbents are often partially occupied or even saturated by the VOCs molecules in practical scenarios, and very few researches have tried to reveal the saturation of ACs during the adsorption processes basing on the characteristic values. Mianowski et al. have previously estimated the surface area of ACs by the iodine number within certain error range, by means of mimicking the BET equation model (Mianowski et al., 2007). The pity is that no adsorption properties were involved in this work. Although the VOCs concentration or pressure drop was also implemented in industrial practice, the prediction accuracy is still doubtful. Therefore, a reasonable and effective method to detect the VOCs adsorption saturation of ACs is now urgently necessitated.

Herein, a series of ACs samples with different quality were collected. Several characteristic values (CTC value, iodine number, total surface area and microporous surface area) were measured for these samples, which were subsequently correlated with the toluene adsorption capacities in presence of different initial concentrations. The results showed that the CTC value is a better characteristic value than the other ones for evaluating the toluene adsorption capacity of ACs, especially under high-concentration situation. Moreover, the toluene adsorption capacities *versus* CTC values over other porous adsorbents (silica gel, zeolites, C@Si) were found to fit well with the same linear regression function basing on the ACs samples, which proved the universal relevance between these two parameters. Thereafter, a model for predicting the CTC value at certain moment and the corresponding saturation of ACs samples was constructed with given parameters (initial CTC value, inlet toluene concentration). Notably, an error within 20% was witnessed between the predicted data and the experimental ones, which strongly validates the accuracy of this model.

1. Materials and methods

1.1. *Chemical and materials*

Toluene (SCR Co. Ltd, > 99.5%), Carbon tetrachloride (RHAWN, > 98%), Iodine (Sangon Biotech, BC grade), B-type silica gel (Qingdao Shuoyuan Silica Technology Co., Ltd.), NaY (SiO_2/Al_2O_3 = 5.5, Nkcatalyst), Naβ (SiO_2/Al_2O_3 = 26, Nkcatalyst), ZSM-5 (Na-type, SiO_2/Al_2O_3 = 26, Nkcatalyst). In addition, a variety of activated carbons from different suppliers were selected for investigation, which were denoted as ACX

(X represents the CTC value of activated carbon). Besides, two types of honeycomb carbons were included, denoted as ACX-HC. The details including CTC value, iodine number, textural properties and supplier of the activated carbons are listed in Appendix A Table S1.1.

1.2. Dynamic adsorption test procedure

The dynamic adsorption test was conducted in a continuous-flow fixed-bed reactor at atmospheric pressure. In each test, 0.3 g or 0.1 g of adsorbents was placed in the U-shaped tube reactor. The toluene feed gas was generated by bubbling the VOCs (toluene) liquid with air in an ice-water bath. The VOCs-containing feed gas was then diluted by certain air flow so that the total flow rate was maintained at 83.3 or 166.6 mL/min (toluene concentration = 10,000, 5000 and 1000 mg/m^3, gas hourly space velocity = 16,660, 33,320 and 99,960 mL/(g·h)). Thereafter, the final feed gases were injected into the U-shaped tube immersed in a 25°C thermostat water bath for adsorption tests. The concentrations of VOCs were continuously measured by automatic sampling into a gas chromatography (Agilent 8860, USA) equipped with a flame ionization detector (FID) and HP-5 column. Meanwhile, the mass before and after the dynamic adsorption tests were both recorded so as to calibrate the VOCs adsorption capacity. The detailed procedure of the dynamic adsorption tests was shown in Appendix A Fig. S2.1. The gas hourly space velocity (GHSV) in the standard state is calculated as Eq. (1):

$$GHSV = \frac{F}{W} \tag{1}$$

where, F (mL/min) is the total gas flow, W (g) is the mass of the adsorbent.

The adsorption capacity of the adsorbent to VOCs is calculated as follows:

$$q = \frac{F \times C_0 \times 10^{-6}}{W}\left[t - \int_0^t \frac{C_i}{C_0} dt\right] \tag{2}$$

where, q (mg/g) is the adsorption capacity, F (mL/min) is the total gas flow, t (min) is the adsorption time, C_0 (mg/m^3) is the inlet mass concentration of VOCs, C_i (mg/m^3) is the outlet mass concentration of VOCs after t min, W (g) is the adsorbent mass.

When the toluene adsorption reaches equilibrium, the adsorption capacity is denoted as q_e (mg/g), and the toluene saturation of the adsorbent can be defined as:

$$S = \frac{q}{q_e} \tag{3}$$

1.3. Carbon tetrachloride adsorption (CTC value) test procedure

The CTC value of activated carbon was tested following the Chinese National Standard (GB/T 7702.13–1997) 'Standard test method for granular activated carbon from coal - Determination of carbon tetrachloride adsorption'. Samples were first dried at 150°C for 2 h (no drying procedure was conducted if the samples had already adsorbed VOCs). After cooling, the samples were loaded into a fixed-bed reactor with a bed height of 10 cm, and then immersed into a 25°C thermostat water bath. Air at a flow rate of 1.5 L/min was then injected into the carbon tetrachloride bubbling flask immersed in a 0°C ice water bath and then into the fixed-bed reactor. After adsorption for 60 min, the mass of the reactor was recorded, followed by measurements at 15-minutes intervals. Adsorption equilibrium was considered achieved when the mass difference between two intervals was less than 0.01 g.

The CTC value was calculated as follows:

$$CTC\ (\%) = \frac{m_e - m_0}{W} \times 100\ (\%) \tag{4}$$

where, m_e (g) is the mass of the reactor after adsorption equilibrium, m_0 (g) is the mass of the reactor before adsorption, W (g) is the mass of the adsorbent.

Notably, CTC_0 (%) represents the CTC value of the fresh sample, while CTC_e (%) represents the CTC value of the sample reaching equilibrium in toluene adsorption. The CTC value of the sample at a given time t during toluene adsorption was labeled as CTC_t (%), and the definition of ΔCTC (%) is:

$$\Delta CTC\ (\%) = CTC_0 - CTC_t \tag{5}$$

Therefore, the ΔCTC value of the sample after equilibrium reached is:

$$\Delta CTC_e\ (\%) = CTC_0 - CTC_e \tag{6}$$

1.4. Iodine number test procedure

The iodine number was conducted by following the Chinese National Standard method (GB/T 7702.7–2023) 'Standard test method for granular activated carbon from coal - Determination of iodine number'. This method is based upon a three-point isotherm. Samples were first dried at 150°C for 2 h. With the estimated iodine number, three samples of varying masses were split using a quadruplicate method. Each sample was then mixed with 10 mL 5 vol.% HCl solution, immersed into a 80°C thermostat water bath for 30 s, and then cooled. Afterward, 100 mL of 0.1 mol/L iodine standard solution was added to the mixture above, followed by shakening for 30 s. The resulting solution was filtered and 50 mL of the filtrate was titrated with 0.1 mol/L sodium thiosulfate standard solution. Afterward, the amount of iodine adsorbed per gram of carbon of the three samples were calculated and the result was linearly fitted to obtain the iodine adsorption isotherm. The iodine adsorption amount at an iodine concentration of 0.02 mol/L was taken as the iodine number of the sample.

1.5. Characterizations

The textual properties of all the samples were collected on a Micromeritics 3-Flex instrument (Micromeritics 3-Flex, USA). All the samples were evacuated at 150°C for 6 h under dynamic vacuum prior to analysis. The specific surface area (S_{total}) of the samples was measured by the BET method according to the nitrogen adsorption isotherms; total pore volume (V_{total}) was calculated by Gurvich-rule at $P/P_0 = 0.95$; The micropores specific surface area (S_{mic}) and micropore volume (V_{mic}) was calculated by the t-Plot method.

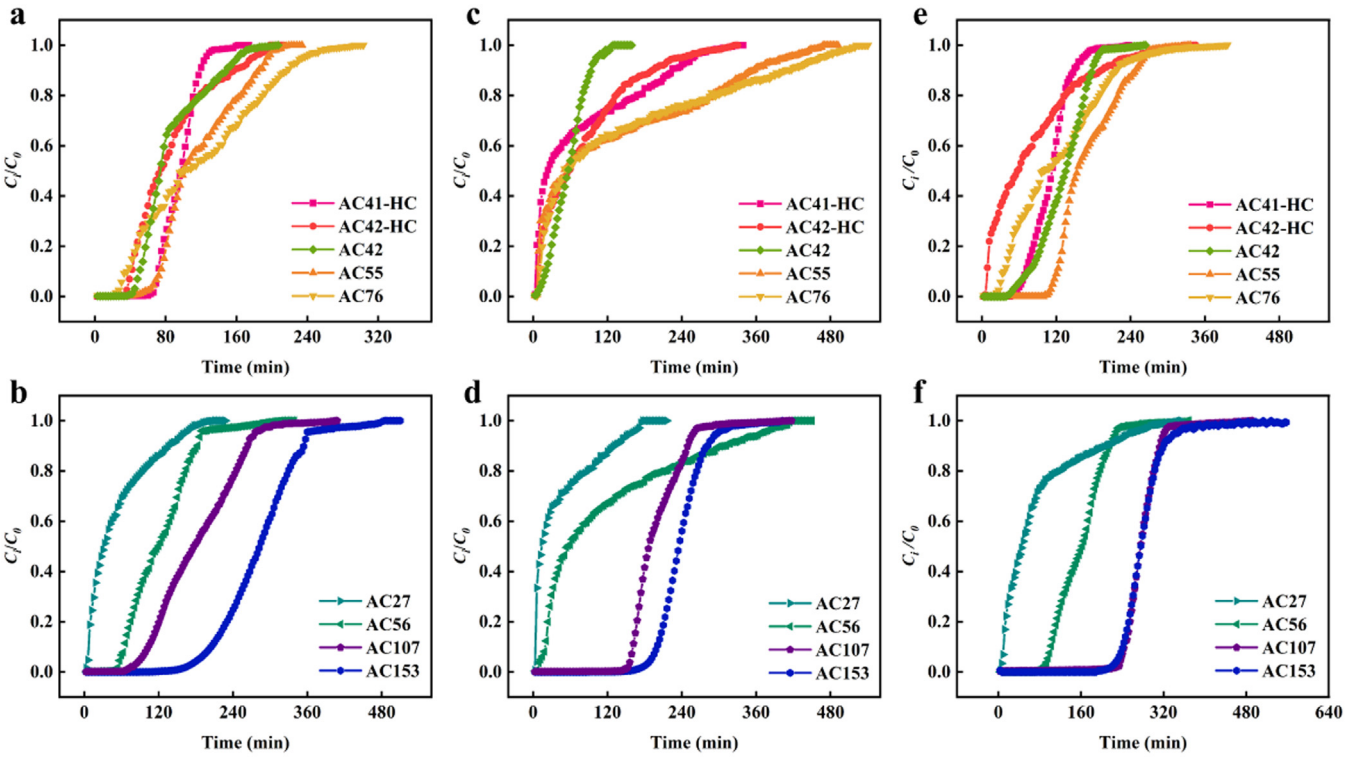

Fig. 1 – Breakthrough curves of activated carbons with different initial toluene concentrations and weight hourly space velocities (GHSV): (a, b) concentration = 10,000 mg/m^3, GHSV = 16,660 mL/(h•g), W = 0.3 g; (c, d) concentration = 5000 mg/m^3, GHSV = 33,320 mL/(h•g), W = 0.3 g; (e, f) concentration = 1000 mg/m^3, GHSV = 99,960 mL/(h•g), W = 0.1 g.

Table 1 – Adsorption capacity of activated carbon to different concentrations of toluene (mg/g).

Adsorbent	Toluene concentration		
	10,000 mg/m^3	5000 mg/m^3	1000 mg/m^3
AC27	143.6	144.8	122.3
AC42	230.4	193.5	214.1
AC55	316.9	345.6	280.6
AC56	332.2	300.3	263.0
AC76	417.9	392.5	296.0
AC107	500.5	499.0	367.9
AC153	764.3	657.9	454.1
AC41-HC	251.4	220.5	181.2
AC42-HC	238.8	217.7	181.1

2. Results and discussion

2.1. *Dynamic toluene adsorption over different ACs samples*

In order to verify the quality of ACs samples from different suppliers, the dynamic toluene breakthrough tests were first conducted (Section 1.2). Considering the great concentration fluctuation of VOCs-containing streams in practice, three different toluene concentrations (10,000 mg/m^3, 5000 mg/m^3 and 1000 mg/m^3) were then adopted in the adsorption tests (Fig. 1). According to the equilibrium adsorption capacities presented in Table 1, significant variations in toluene adsorption performance over different ACs samples were observed. As mentioned above, characteristic values are frequently used to represent the adsorption properties of ACs sample. For this reason, the iodine number, CTC value, ash content, total specific surface area and microporous specific surface area were measured beforehand and summarized in Appendix A Table S1.1. Accordingly, ACs samples with higher iodine numbers, CTC values or surface areas also translate to greater toluene equilibrium adsorption capacities, regardless of the variation of toluene concentrations, which indicated strong correlation between adsorption capacity and characteristic values (Appendix A Table S1.1 and 2).

2.2. *Correlation between adsorption capacity and characteristic values*

Although the adsorption capacity has shown close association with the characteristic values, further researches were

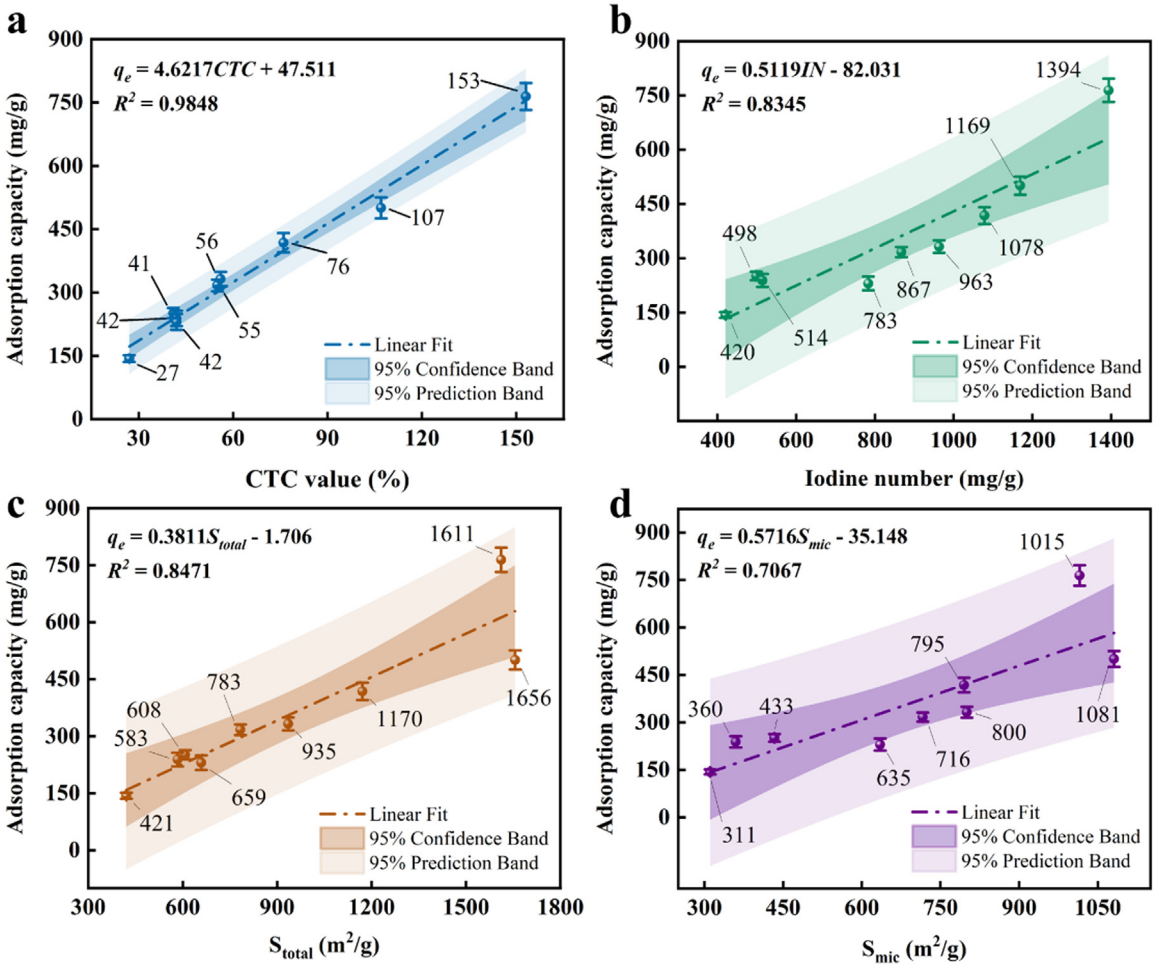

Fig. 2 – Linear regression of toluene adsorption capacity at 10,000 mg/m^3 initial concentration with (a) CTC value, (b) iodine number, (c) total specific surface area (S_{total}) and (d) microporous specific surface area (S_{mic}) (CTC value refers to the carbon tetrachloride adsorption rate). The confidence band represents the uncertainty in an estimate of a curve or function, while the prediction band intends to describe the value of a new data-point subject to noise, so the prediction bands would be generally wider than the confidence bands.

still necessary to screen out the most appropriate characteristic value. Therefore, linear regression analyses were then conducted for the toluene equilibrium adsorption capacity under varied concentrations *versus* the aforementioned characteristic values, *i.e.* iodine number, CTC value, total specific surface area, and micropore specific surface area. As demonstrated, when exposed to high-concentration toluene, CTC value exhibited relatively higher correlation ($R^2 = 0.9848$) with toluene adsorption capacity, when compared to those of total specific surface area ($R^2 = 0.9491$), iodine number ($R^2 = 0.8345$), and micropore specific surface area ($R^2 = 0.7067$), etc. (Fig. 2, Appendix A Table S3.1). Thereby, CTC value is obviously the most proper indicative value for toluene adsorption capacity in high-concentration circumstance over ACs adsorbents, regardless of the ACs sources or forms (particle or honeycomb). As the toluene concentration decreased, however, the correlation of the CTC value with the toluene adsorption capacity gradually deteriorated, while the correlation of the iodine number and surface area became stronger (Appendix A Fig. S3.1 and S3.2, Table S3.1). A possible explanation may be that the iodine number was tested in a diluted aqueous iodine solution which resembled the toluene adsorption test conditions, while the CTC value was measured using high-concentration carbon tetrachloride vapor, which greatly deviated from the toluene adsorption environment. Notably, even though the correlation between the CTC value and the toluene adsorption capacity was weakened with the reduction of toluene concentration, the correlation coefficients between them were still high ($R^2 > 0.92$), which evidenced that the CTC value could be an excellent candidate to characterize the toluene adsorption capacity in a broad concentration range.

To further reveal the reason for the association between the CTC value and the toluene adsorption capacity, the BET equation was modified using different probe molecules. Generally, the BET specific surface area could be calculated as follows:

$$S_{BET} = a_m \times N \times \omega_{N_2} \quad (7)$$

where, a_m (mol/g) is the monolayer adsorption capacity; N (mol^{-1}) is the Avogadro's number ($N = 6.023 \times 10^{23}$ mol^{-1});

Table 2 – Radius comparison for different adsorbate molecules.

Adsorbate	van der Waals radius (Å)	Radius according to Eq. (11) (Å)
N_2	1.5	2.2
I_2	2.2	2.4
CCl_4	3.5	3.4
toluene (10,000 mg/m^3)	2.9	3.5
toluene (1000 mg/m^3)	2.9	4.3

ω_{N_2} is the surface area occupied by one adsorbate molecule in the complete monolayer coverage, ($\omega_{N_2} = 0.162 \times 10^{-18}$ m^2 at 77 K). Apparently, the BET specific surface area could also be expressed by the monolayer adsorption capacity of different adsorbates, taking the carbon tetrachloride as an example:

$$S_{CTC} = \frac{CTC \times 10^{-2}}{M_{CCl_4}} \times N \times \omega_{CCl_4} \quad (8)$$

$$S_{BET} = \frac{CTC \times 10^{-2}}{M_{CCl_4}} \times N \times \omega_{CCl_4} + \Delta S \quad (9)$$

where, CTC (%) represents the measured CTC value assuming that all the adsorbed carbon tetrachloride molecules occupied monolayer of ACs samples, ΔS (m^2/g) is the error term, which is the same for different ACs samples, and M_{CCl_4} (m^2) is the molecular weight.

$$S_{BET} = 15.766 \times CTC - 26.6 \quad (10)$$

Combining the fitting Eq. (10) of carbon tetrachloride and S_{BET} equation, it could be yielded that $\omega_{CCl_4} = 0.4026 \times 10^{-18}$ m^2.

Assuming a surface coverage by densely packed hexagonal lattices according to previous publication, the molecular radius could be derived from the radius attached to the hexagonal circle (Appendix A Fig. S3.3) (Mianowski et al., 2007):

$$r = \sqrt{\frac{\sqrt{3} \times \omega}{6}} \quad (11)$$

where, r (Å) represents the radius of the circle inscribed into the hexagon (Appendix A Fig. S3.3), ω (Å^2) is the surface area occupied by one adsorbate molecule in the complete monolayer coverage.

Following the same fitting procedure, the simulated radius values of different probe molecules were calculated and summarized in Table 2. Except for the toluene molecules under low concentration, the calculated radius values were all observed to approach their van der Waals radius values. Besides, the calculated radius for iodine was found close to the previously reported value (2.5 Å) (Mianowski et al., 2007), which verified the feasibility of the hypothesis. The larger radius of toluene under low concentration may be caused by the incomplete monolayer adsorption, which gave rise to higher occupying area of each toluene molecule. Noticeably, the carbon tetrachloride radius deviated to a similar extent with the toluene radius at high concentration, quite probably due to their approximate van der Waals radius values, which well manifested the reason behind the strong correlation between the CTC value and the toluene adsorption capacity, especially at high concentrations.

2.3. *Correlation between the CTC value and toluene adsorption saturation*

Since the CTC value has already been proven the most suitable indicator for the toluene adsorption capacity, a remaining problem is whether the saturation of ACs samples partially occupied by VOCs molecules could be predicted. Herein, a mathematical model of toluene adsorption capacity over ACs samples under high concentration (10,000 mg/m^3) was first built upon the CTC values due to the strong correlation between these two variables. To obtain ACs samples with different saturation, toluene adsorption experiments were performed in parallel multiple times. Several adsorption time points (t) were selected basing on the breakthrough curves, and saturation was calculated using Eq. (3) to achieve even distribution between 0 and 1. Besides, the ACs samples were immediately taken out at the selected time points (t), followed by CTC value measurements directly.

As shown in Fig. 3a, with the initial CTC_0 values within the range from 27% to 153%, the saturation of the ACs samples all exhibited a linear relationship with the ΔCTC values, even though these ACs samples are from diverse suppliers (which means different raw materials and manufacture procedures). These results clearly demonstrates that the CTC values can somewhat represent the remaining adsorption capacity, or saturation, of ACs samples after VOCs adsorption. Here the ΔCTC values were adopted, instead of CTC values, to build the corresponding mathematical model of toluene adsorption saturation, so as to get a proportional function form (because $S = 0$ for the fresh ACs samples), as follows:

$$S = K \times (CTC_0 - CTC_t) = K \times \Delta CTC \quad (12)$$

where, CTC_0 (%) is the initial CTC value of fresh sample, CTC_t (%) is the CTC value at adsorption time t, K is the saturation slope.

Obviously, the saturation slope K in Eq. (12) is quite crucial since it stands for the descending rate of toluene adsorption saturation. In this case, the parameter K could be simply derived using the CTC_0 value of the fresh sample and the CTC value reaching equilibrium (CTC_e) ($S = 1$ at this moment):

$$K = \frac{1}{(CTC_0 - CTC_e)} = \frac{1}{\Delta CTC_e} \quad (13)$$

Although the linear correlation between the toluene adsorption saturation and the ΔCTC values has been established, it is essential to verify if the AC samples with similar CTC_0 values but different origins still conform to the same equation. With this regard, AC samples with similar CTC_0 values were picked up for further investigation. As indicated in Fig. 3b, for samples with similar CTC_0 values, their linear regression curves and saturation slope K values were also resembled (Appendix A Table S3.2). This phenomenon strongly validated

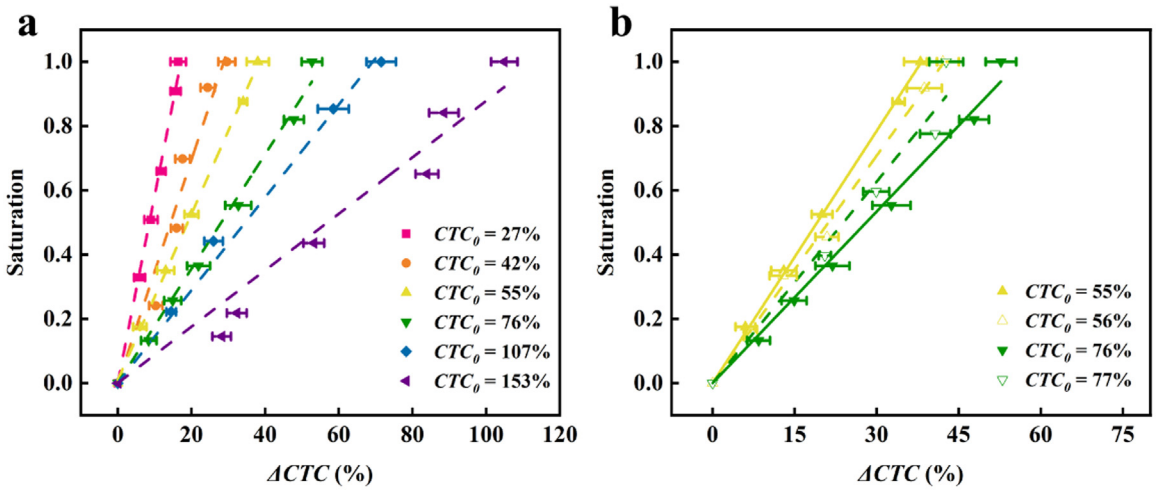

Fig. 3 – Linear regression of toluene saturation rate (%) at 10,000 mg/m^3 initial concentration *versus* ΔCTC values in presence of (a) different initial CTC values (CTC_0) and (b) similar CTC_0 values. (The definition of ΔCTC and CTC_0 were classified in Section 1.3).

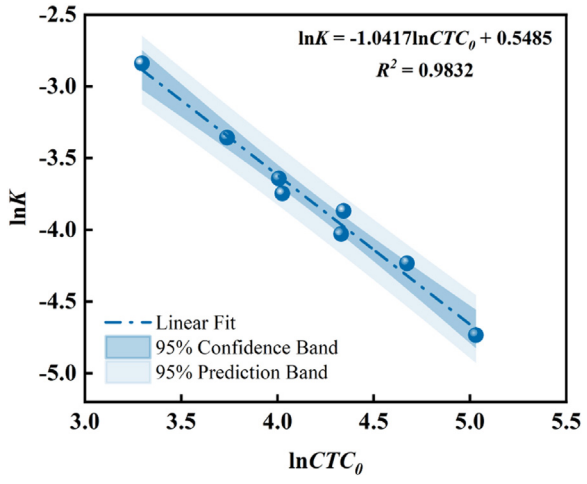

Fig. 4 – Logarithmic linear regression of slope *K* values in Fig. 3a according to Eq. (12) *versus* different initial CTC_0 values.

that the equation above could be extensively used to predict the saturation of diverse ACs samples.

2.4. *Modeling of toluene saturation slope K and the initial CTC value (CTC_0)*

According to Fig. 3a, it could be noted that the initial CTC_0 values of the ACs samples showed a negative correlation with the toluene saturation slope *K*. In order to unravel the relationship between CTC_0 value and parameter *K*, a mathematical model for these two variables was constructed as well. As depicted in Fig. 4, the logarithm of parameter *K* (ln*K*) showed a negative linear correlation to the logarithm of different CTC_0 values ($\ln CTC_0$), as plotted below.

$$\ln K = \alpha \times \ln(CTC_0) + \beta \quad (14)$$

In summary, given a fixed toluene concentration of 10,000 mg/m^3, a linear correlation between the toluene adsorption saturation and the ΔCTC values has already been proven. Meanwhile, the saturation slope *K* was also found to follow a logarithmic linear correlation with the initial CTC_0 values. Given this, it is reasonable to surmise that the saturation slope *K* corresponding to any CTC_0 value in the range from 27% to 153%, could also be calculated by this way.

2.5. *Visual modelling of CTCe value and toluene saturation rate*

Even though a feasible method has been put forward in Section 2.3-2.4 to calculate the toluene adsorption saturation under a constant toluene concentration of 10,000 mg/m^3, it should be noted that the VOCs adsorption typically occurs under much lower concentrations, and the adsorption performance of ACs varies significantly with their quality and VOCs concentrations. To tackle this issue, the dynamic breakthrough tests were conducted on a series of ACs samples under different initial toluene concentrations (Appendix A Section S2). Since the toluene saturation slope *K* and ΔCTC_e value could serve as indicators for saturation changes according to Eq. (12), the ΔCTC_e values were then plotted against the initial toluene concentrations. As shown in Fig. 5a, the ΔCTC_e values generally increased with the increase of toluene concentrations. This is because the toluene adsorption capacity increased with the enhancement of toluene concentration, which resulted in a lower CTC value when reaching equilibrium (so $\Delta CTC_e = CTC_0 - CTC_e$ got higher). Meanwhile, the ΔCTC_e values of different ACs samples (CTC_0 = 27%, 56%, 107%) all showed a linear correlation with the inlet toluene concentrations (C_0), which implied the dependence of toluene adsorption saturation on the inlet C_0 values.

In order to predict the saturation state, the database has to be expanded basing on the collected data, typically by a interpolation method. To verify the accuracy of the interpolation, the predicted saturated ΔCTC_e values with fixed CTC_0 (42%

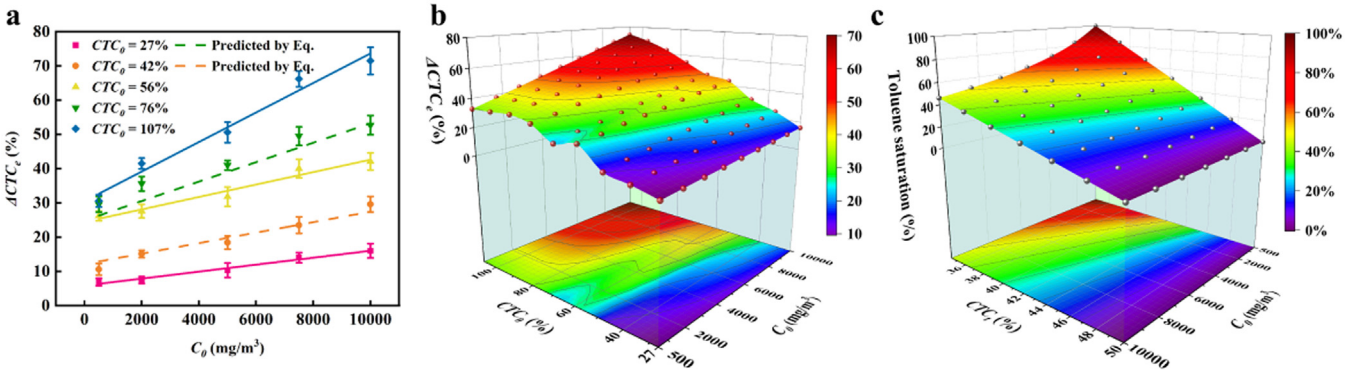

Fig. 5 – (a) Linear regression of ΔCTC_e values under equilibrium with different initial toluene concentrations (C_0) in presence of different initial CTC_0 values, along with the prediction of ΔCTC_e values basing on the collected data; (b) the visual modelling of ΔCTC_e values under equilibrium against C_0 and CTC_0 values; (c) the visual modelling of toluene saturation rate (%) against C_0 and CTC_t values, given a fixed CTC_0 value of 50%.

Table 3 – Comparison of predicted saturated CTC_e in Fig. 5a with experimental data collected under different CTC_0 values and initial toluene concentrations (C_0).

CTC_0	C_0 (mg/m^3)	Predicted CTC_e	Experimental CTC_e	Error
42%	10,000	14.6%	12.4%	17.7%
	7500	18.4%	18.5%	0.7%
	5000	22.2%	23.6%	6.0%
	2000	26.8%	26.9%	0.4%
	500	29.2%	31.4%	7.2%
76%	10,000	22.8%	23.5%	2.9%
	7500	29.8%	26.5%	12.6%
	5000	36.9%	35%	5.4%
	2000	45.4%	40.4%	12.5%
	500	49.8%	46.4%	7.3%

CTC_0: the carbon tetrachloride adsorption value of the fresh sample; CTC_e: the carbon tetrachloride adsorption value of the sample reaching equilibrium in toluene adsorption.

and 76%) and C_0 (500–10,000 mg/m^3) values were compared to the experimental data (Table 3). A detailed interpolation example was exhibited in Appendix A Section S4. Briefly, the interpolation was conducted by the logarithmic linear regression of slope K values (obtained from ΔCTC_e values) against the logarithm of different CTC_0 values, just as Eq. (14) and Fig. 4. Noticeably, the predicted CTC_e values were generally within 18% error of the measured ones (Table 3), and no obvious association has been witnessed between the relative errors and the CTC_0 or the inlet toluene concentrations (C_0). This means, the interpolation method is applicable at least in the toluene concentration range from 500 to 10,000 mg/m^3 and CTC_0 value range from 27% to 107%. As such, a visual modelling of ΔCTC_e values under toluene adsorption equilibrium against C_0 and CTC_0 values was constructed (Fig. 5b).

Because the accuracy of the interpolation method has been testified above, it could then be concluded that the toluene saturation slope K follows a logarithmic linear correlation with the CTC_0 values in a broad concentration range, similar to Eq. (14). In other words, each C_0 variable correspond to a specific α and β parameter, which could be interpreted as the following function:

$$\alpha = f(C_0);\ \beta = f(C_0) \tag{15}$$

The calculation process for parameters α and β was referred in Appendix A Section S4. Next to that, the toluene saturation could be interpreted as a function of the inlet toluene concentration C_0, CTC_0 and the adsorption time (or CTC_t value):

$$S = f(C_0,\ CTC_0,\ CTC_t) \tag{16}$$

Combining Eqs. (14) and (12), the toluene saturation could be described as follows:

$$S = e^{\alpha \times \ln(CTC_0)+\beta} \times (CTC_0 - CTC_t) \tag{17}$$

Since each C_0 variable correspond to a specific α and β parameter, a visual modelling of toluene saturation against C_0 and CTC_t values was constructed basing upon Eq. (17), assuming that the initial CTC_0 value of 50% (Fig. 5c). Given the fast and simple CTC value determination procedure, the satura-

Table 4 – Comparison of predicted & experimental adsorption capacity on porous adsorbents[a].

Samples	CTC_0 value[b]	Adsorption capacity predicted by equation (mg/g)	Experimental adsorption capacity[c] (mg/g)	Error
B Type Silica	10.2%	94.7	82.4	14.9%
NaY	40.5%	234.7	212.7	10.3%
ZSM-5	10.2%	94.7	74.5	27.1%
Naβ	16.7%	124.7	159.5	21.8%
C@Si[d]	17.5%	128.4	110.9	15.8%

[a] According to equation in Fig. 2a. [b] CTC_0: the carbon tetrachloride adsorption value of the fresh sample. [c]Experimental condition: C_0=10,000 mg/m^3, *GHSV*=16,660 mL/(h·g), W = 0.3 g. [d]The preparation of C@Si composite was referred in Appendix A Section S1.2.

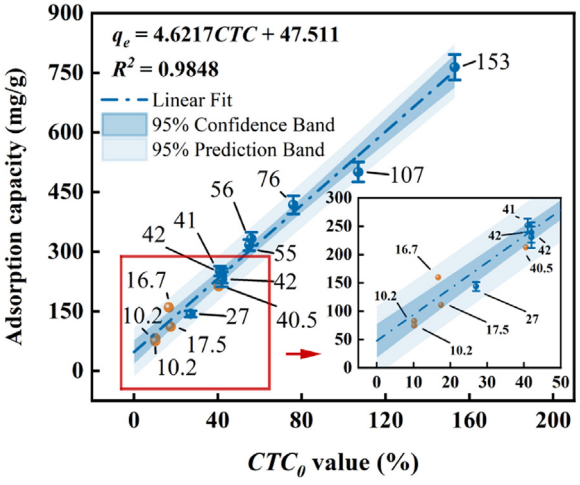

Fig. 6 – The matching of toluene adsorption capacity of other porous adsorbent materials to the linear regression plot in Fig. 2a. (The orange dots represent the experimental data of other porous adsorbent materials. Experimental condition: C_0 = 10,000 mg/m^3, *GHSV* = 16,660 mL/(h•g), W = 0.3 g).

tion of the ACs samples can then be quickly and accurately estimated.

2.6. *Extension of correlation to other porous adsorbents*

Currently, the CTC values are only used to evaluate the adsorption performances of ACs samples. In order to certify whether the equation is still applicable to other porous adsorbents, a series of conventional porous materials (*e.g.* zeolites, silica gel and C@Si composite) were further selected for study. The equilibrium adsorption capacities of toluene for five different adsorbents in presence of a fixed toluene concentration of 10,000 mg/m^3 were measured along with their CTC_0 values, as listed in Table 4. Besides, the equilibrium toluene adsorption capacities were predicted using the regression equation in Fig. 2a for comparison.

As shown in Table 4, the equilibrium toluene adsorption capacities predicted by the equations were within 15% error of the measured values for B-type silica gel, C@Si composites and NaY zeolite, and within 30% error for ZSM-5 and Naβ zeolites. With the additional five adsorbents, the correlation between the CTC_0 value and the equilibrium adsorption amount of toluene was still acceptable, and then the dependence between the CTC value and the equilibrium toluene adsorption capacities could be assumed to extend to other adsorbents except for ACs (Fig. 6). However, tests over more types of adsorbents still needs to be carried out, due to the wide variety of adsorbents and the complexity of the factors affecting adsorption.

3. Conclusions

As described, the dynamic adsorption capacity toward toluene over a series of activated carbon samples were linearly correlated with several different characteristic values, *i.e.* iodine number, CTC value, total specific surface area, and micropore specific surface area. Therein, CTC value showed a relatively stronger linear correlation with the toluene adsorption capacity, especially in high-concentration circumstance, in despite of the carbon sources and forms. When extending to other porous adsorbents, their toluene adsorption amounts and initial CTC values fitted well with the same equation derived from the activated carbon samples, which indicated the broad applicability of the CTC value in predicting adsorption capacity. Basing upon the correlation between the toluene adsorption capacity and CTC value, mathematical and visual models were constructed to predict the CTC value in equilibrium, as well as the toluene saturation at specific moment over diverse activated carbons. By comparing the experimental and predicted adsorption behaviors, the prediction was generally within 18% error of the measurement, at least in the toluene concentration of 500–10,000 mg/m^3 and CTC_0 value range of 27%–107%. These results evidence that the CTC value can serve as an excellent indicator to characterize the toluene adsorption performance (capacity and saturation) of activated carbon and other porous adsorbents, and thereby, the fast and accurate estimation of the activated carbon quality and adsorption saturation state can now be realized.

Declaration of Competing Interest

The authors declare that they have no known competing financial interests or personal relationships that could have appeared to influence the work reported in this paper.

Acknowledgments

This work was supported by the Key Research and Development Projects in Zhejiang Province (Nos. 2023C03127, 2024C03114, 2024C03108), the Natural Science Foundation of China (Nos. 22208300, 22078294), the Natural Science Foundation of Zhejiang Province (No. LQ23B060007), the Fundamental Research Funds for the Provincial Universities of Zhejiang (No. RF-A2023004) and Zhejiang Provincial Postdoctoral Science Foundation (No. ZJ2023145).

Appendix A Supplementary data

Supplementary material associated with this article can be found in the online version at doi:10.1016/j.jes.2024.04.039.

References

Algrim, L.B., Pagonis, D., de Gouw, J.A., Jimenez, J.L., Ziemann, P.J., 2020. Measurements and modeling of absorptive partitioning of volatile organic compounds to painted surfaces. Indoor Air 30 (4), 745–756.

Bradley, R.H., 2011. Recent developments in the physical adsorption of toxic organic vapours by activated carbons. Adsorpt. Sci. Technol. 29 (1), 1–28.

Dai, Z., Li, D., Ao, Z., Wang, S., An, T., 2021. Theoretical exploration of VOCs removal mechanism by carbon nanotubes through persulfate-based advanced oxidation processes: adsorption and catalytic oxidation. J. Hazard. Mater. 405, 124684.

Garba, S., 2016. Surface modification of activated carbon for improved iodine and carbon tetrachloride adsorption. Am. J. Chem. 6, 74–79.

Goswami, R., Dey, A., 2022. Activated carbon from agricultural residues: a review. Desalin. Water Treat. 278, 283–292.

Hao, X., Xiafan, X., Liubiao, C., Jia, G., Junjie, W., 2021. A novel cryogenic condensation system based on heat-driven refrigerator without power input for volatile organic compounds recovery. Energy Convers. Manage. 238, 114157.

He, C., Cheng, J., Zhang, X., Douthwaite, M., Pattisson, S., Hao, Z., 2019. Recent advances in the catalytic oxidation of volatile organic compounds: a review based on pollutant sorts and sources. Chem. Rev. 119 (7), 4471–4568.

Ji, J., Xu, Y., Huang, H., He, M., Liu, S., Liu, G., et al., 2017. Mesoporous TiO_2 under VUV irradiation: enhanced photocatalytic oxidation for VOCs degradation at room temperature. Chem. Eng. J. 327, 490–499.

Juhola, A.J., 1975. Iodine adsorption and structure of activated carbons. Carbon N Y 13 (5), 437–442.

Li, X., Zhang, L., Yang, Z., Wang, P., Yan, Y., Ran, J., 2020. Adsorption materials for volatile organic compounds (VOCs) and the key factors for VOCs adsorption process: a review. Sep. Purif. Technol. 235, 116213.

Liang, Z., Yu, Y., Sun, B., Yao, Q., Lin, X., Wang, Y., et al., 2024. The underappreciated role of fugitive VOCs in ozone formation and health risk assessment emitted from seven typical industries in china. J. Environ. Sci. 136, 647–657.

Lin, Q., Gao, Z., Zhu, W., Chen, J., An, T., 2023. Underestimated contribution of fugitive emission to VOCs in pharmaceutical industry based on pollution characteristics, odorous activity and health risk assessment. J. Environ. Sci. 126, 722–733.

Liu, Y., Peyravi, A., Dong, X., Hashisho, Z., Zheng, S., Chen, X., et al., 2023. Effect of microstructure in mesoporous adsorbents on the adsorption of low concentrations of VOCs: an experimental and simulation study. J. Hazard. Mater. 458, 131934.

Mianowski, A., Owczarek, M., Marecka, A., 2007. Surface area of activated carbon determined by the iodine adsorption number. Energy Sources Part A 29 (9), 839–850.

Ouzzine, M., Romero-Anaya, A.J., Lillo-Ródenas, M.A., Linares-Solano, A., 2019. Spherical activated carbons for the adsorption of a real multicomponent VOC mixture. Carbon N Y 148, 214–223.

Rao, R., Ma, S., Gao, B., Bi, F., Chen, Y., Yang, Y., et al., 2023. Recent advances of metal-organic framework-based and derivative materials in the heterogeneous catalytic removal of volatile organic compounds. J. Colloid Interface Sci. 636, 55–72.

Shen, Y., 2023. Biomass-derived porous carbons for sorption of volatile organic compounds (VOCs). Fuel 336, 126801.

Shi, Q., Kang, D., Wang, Y., Zhang, X., 2023. Emission control of toluene in iron ore sintering using catalytic oxidation technology: a critical review. Catalysts 13 (2), 429.

Soni, V., Singh, P., Shree, V., Goel, V., 2018. Effects of VOCs on human health. In: Sharma, N, Agarwal, A K, Eastwood, P, Gupta, T, Singh, AP (Eds.), Air Pollution and Control. Springer Singapore, Singapore, pp. 119–142.

Sun, P., Cheng, L., Chen, S., Xie, M., Dong, F., Dong, X., 2024. Nickel foam based monolithic catalyst supporting transition metal oxides for toluene combustion: experimental and theoretical study of interfacial synergistic oxidation and water resistance. Chem. Eng. J. 483, 149176.

Tan, R., Guo, S., Lu, S., Wang, H., Zhu, W., Yu, Y., et al., 2023. Characteristics and secondary organic aerosol formation of volatile organic compounds from vehicle and cooking emissions. Atmosphere (Basel) 14 (5), 806.

Wang, H., Xu, J., Liu, X., Sheng, L., 2021. Preparation of straw activated carbon and its application in wastewater treatment: a review. J. Cleaner Prod. 283, 124671.

Wei, X., Wu, S., Liu, P., Huang, S., Li, X., Yang, J., et al., 2023. Characterization of physicochemical properties of activated carbons prepared from penicillin mycelial residues and its adsorption properties for VOCs. J. Environ. Chem. Eng. 11 (3), 109733.

Wu, X., Lin, Y., Wang, Y., Wu, S., Yang, C., 2023. Volatile organic compound removal via biofiltration: influences, challenges, and strategies. Chem. Eng. J. 471, 144420.

Xiang, W., Zhang, X., Chen, K., Fang, J., He, F., Hu, X., et al., 2020. Enhanced adsorption performance and governing mechanisms of ball-milled biochar for the removal of volatile organic compounds (VOCs). Chem. Eng. J. 385.

Yang, C., Miao, G., Pi, Y., Xia, Q., Wu, J., Li, Z., et al., 2019. Abatement of various types of VOCs by adsorption/catalytic oxidation: a review. Chem. Eng. J. 370, 1128–1153.

Yang, W., Kim, M.-Y., Polo-Garzon, F., Gong, J., Jiang, X., Huang, Z., et al., 2023. CH_4 combustion over a commercial Pd/CeO_2-ZrO_2 three-way catalyst: impact of thermal aging and sulfur exposure. Chem. Eng. J. 451, 138930.

Ye, Q., Chen, Y., Li, Y., Jin, R., Geng, Q., Chen, S., 2023. Management of typical VOCs in air with adsorbents: status and challenges. Dalton Trans 52 (35), 12169–12184.

Yu, B., Deng, H., Lu, Y., Pan, T., Shan, W., He, H., 2024. Adsorptive interaction between typical VOCs and various topological zeolites: mixture effect and mechanism. J. Environ. Sci. 136, 626–636.

Zhang, W., Li, G., Yin, H., Zhao, K., Zhao, H., An, T., 2022. Adsorption and desorption mechanism of aromatic VOCs onto porous carbon adsorbents for emission control and resource recovery: recent progress and challenges. Environ. Sci.: Nano 9 (1), 81–104.

Zhang, X., Gao, S., Fu, Q., Han, D., Chen, X., Fu, S., et al., 2020a. Impact of VOCs emission from iron and steel industry on regional O_3 and PM2.5 pollutions. Environ. Sci. Pollut. Res. 27 (23), 28853–28866.

Zhang, Z., Jiang, C., Li, D., Lei, Y., Yao, H., Zhou, G., et al., 2020b. Micro-mesoporous activated carbon simultaneously possessing large surface area and ultra-high pore volume for efficiently adsorbing various VOCs. Carbon 170, 567–579.

Zhang, Z., Jiang, Z., Shangguan, W., 2016. Low-temperature catalysis for VOCs removal in technology and application: a state-of-the-art review. Catal. Today 264, 270–278.

Zhou, Q., Zhang, L., Chen, J., Luo, Y., Zou, H., Sun, B., 2016. Enhanced stable long-term operation of biotrickling filters treating VOCs by low-dose ozonation and its affecting mechanism on biofilm. Chemosphere 162, 139–147.

Zhu, L., Shen, D., Luo, K.H., 2020. A critical review on VOCs adsorption by different porous materials: species, mechanisms and modification methods. J. Hazard. Mater. 389, 122102.